

Polyelectrolyte Nanoparticles with High Drug Loading Enhance the Oral Uptake of Hydrophobic Compounds

Woei Ping Cheng,[†] Alexander I. Gray,[†] Laurence Tetley,[‡] Thi Le Bich Hang,[†]
Andreas G. Schätzlein,[§] and Ijeoma F. Uchegbu^{*†}

Department of Pharmaceutical Sciences, Strathclyde Institute for Biological Sciences Building, University of Strathclyde, 27 Taylor Street, Glasgow G4 0NR, U.K., Electron Microscopy Unit, Institute of Biomedical & Life Sciences, University of Glasgow, G12 8QQ, Lanark, Scotland, and Cancer Research UK Centre for Oncology and Applied Pharmacology, Beatson Laboratories, University of Glasgow, Switchback Road, Garscube Estate, Glasgow G61 1BD, U.K.

Received February 10, 2006

In the pharmaceutical industry, orally active compounds are required to have sufficient water solubility to enable dissolution within the gastrointestinal tract prior to absorption. Limited dissolution within the gastrointestinal tract often reduces the bioavailability of hydrophobic drugs. To improve gastrointestinal tract dissolution, nonaqueous solvents are often used in the form of emulsions and microemulsions. Here, we show that oil-free polyelectrolyte nanosystems (micellar dispersions and 100–300 nm particles) prepared from poly(ethylenimines) derivatized with cetyl chains and quaternary ammonium groups are able to encapsulate high levels of hydrophobic drug (0.20 g of drug per g of polymer) for over 9 months, as demonstrated using cyclosporine A (log *P* = 4.3). The polyelectrolytes facilitate the absorption of hydrophobic drugs within the gastrointestinal tract by promoting drug dissolution and by a hypothesized mechanism involving paracellular drug transport. Polyelectrolyte nanoparticle drug blood levels are similar to those obtained with commercial microemulsion formulations. The polyelectrolytes do not promote absorption by inhibition of the P-glycoprotein efflux pump.

Introduction

High levels of hydrophobic compounds are often required within oil-free aqueous media in both the pharmaceutical and food industries. In the pharmaceutical industry, the need to improve the aqueous solubility of drugs is particularly acute when formulating medicines, as low drug solubility in aqueous media hampers the ability of drugs to be administered via the intravenous route and also limits oral drug bioavailability. Drug molecules are becoming more lipophilic, and it is estimated that 40% of new chemical entities fail in development because of adverse physical properties such as poor aqueous solubility.¹ Strategies which enable drugs to be solubilized within hydrophobic nanodomains, which are in turn dispersed within aqueous media, for example, solubilization within micelles, are needed. Traditional techniques such as the use of cosolvents,² low molecular weight surfactant micelles,³ emulsions,² and cyclodextrins² often require excipient/drug weight ratios of at least 15:1 and often as much as 1000:1 and are also not always effective. In the current article, we report that amphiphilic poly(ethylenimines) (PEIs)⁴ are able to efficiently encapsulate hydrophobic drugs within either micelles or stable 200–300 nm nanoparticles in aqueous dispersions at polymer/drug ratios of as little as 5:1 and also that these particles retain the drug as a colloidal dispersion for over 9 months. Also, here we show that, by facilitating the aqueous dissolution of hydrophobic drugs, these amphiphilic polyelectrolytes enhance the oral absorption of such drugs.

The ability of these polyelectrolytes to disperse a hydrophobic drug within aqueous media and promote the oral absorption of

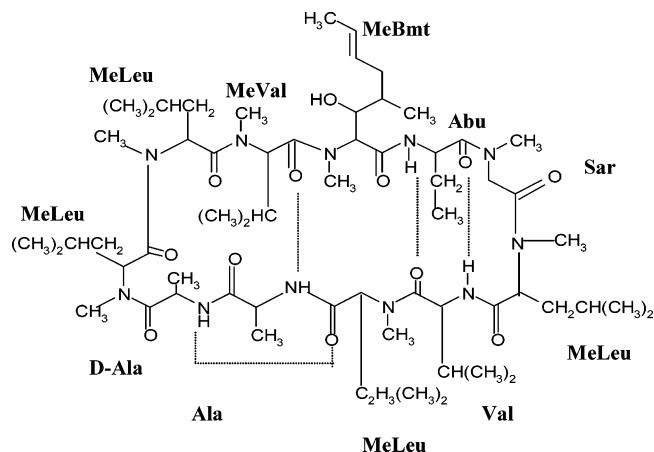


Figure 1. Chemical structure of cyclosporine A (CsA). Dotted lines indicate intramolecular hydrogen bonding.

same is exemplified here with the model drug cyclosporine A (CsA, Figure 1). CsA, a cyclic undecapeptide lipophilic immunosuppressant drug used to treat transplant and autoimmune disease patients, is currently administered orally as a microemulsion formulation (Neoral).⁵ CsA has a molecular weight of 1202 Da, a very low intrinsic water solubility (19.9 $\mu\text{g mL}^{-1}$ at 25 °C)⁶ and a log *P* (octanol/water) of 4.3 at room temperature.⁷

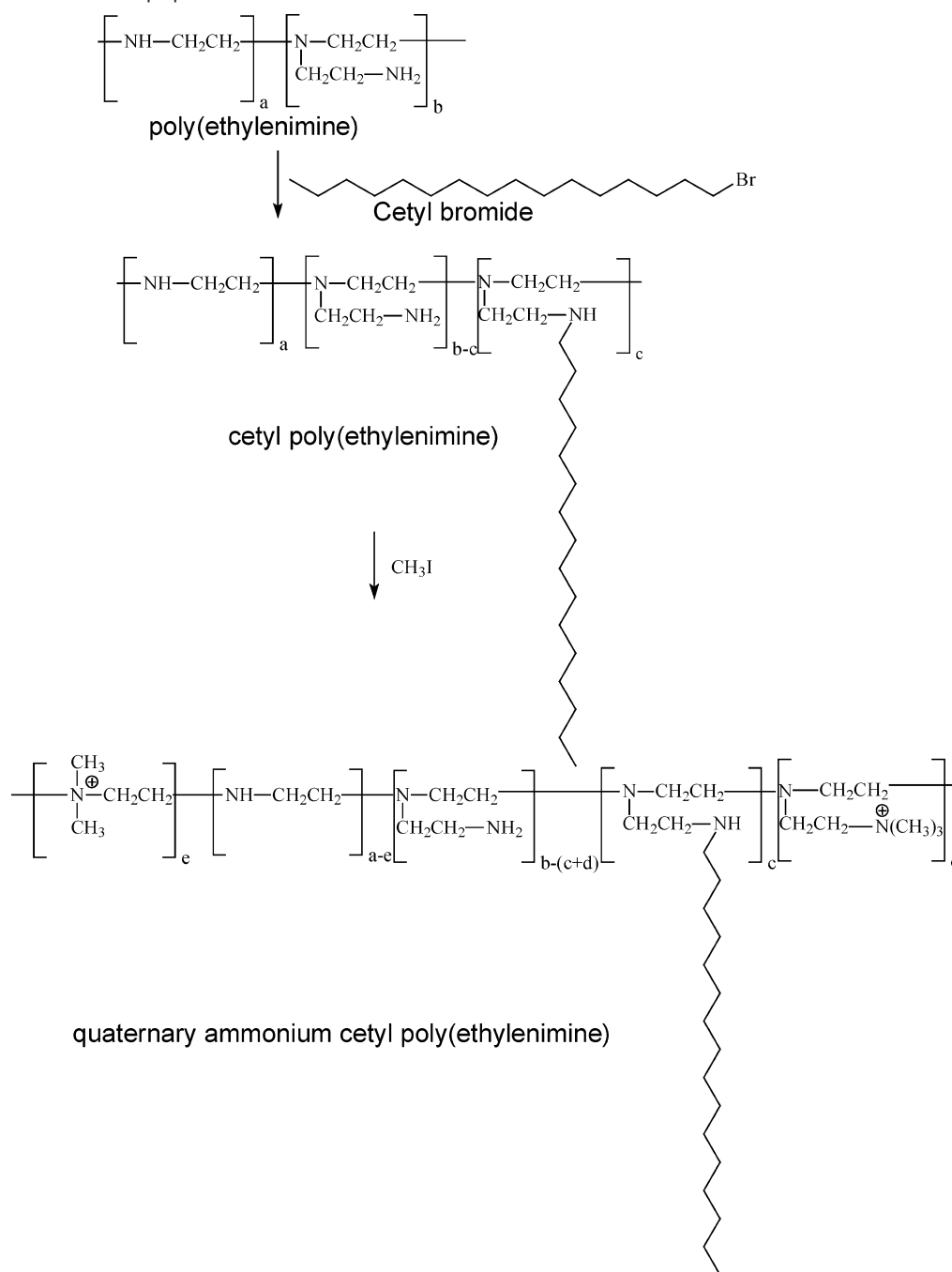
Methods

Polymer Synthesis. *Synthesis of Cetyl Poly(ethylenimine) (CPEI).* This was carried out as shown in Scheme 1 by adapting a previously reported method used for the synthesis of cetyl linear PEI.⁴ However, in this case, the starting material was branched PEI. Branched PEI was reacted with cetyl bromide (both from Sigma Aldrich, Co., U.K.) in

[†] University of Strathclyde.

[‡] Institute of Biomedical & Life Sciences, University of Glasgow.

[§] Beatson Laboratories, University of Glasgow.

Scheme 1. Synthesis of PEI Amphiphiles**Table 1.** Synthesis of Quaternary Ammonium Cetyl Polyethylenimine

| polymer sample | PEI molecular weight (kDa) | monomer, cetyl bromide molar ratio | number of quaternization steps | mol % cetylation (Ct) | mol % quaternization (Q) | hydrophilicity index (HI = Q/Ct) |
|-------------------|----------------------------|------------------------------------|--------------------------------|--|--|----------------------------------|
| C ₂₅ | 25 | 1:0.15 | 0 | 5.0 (5.2, 4.7, <i>n</i> = 2) | 0 | 0 |
| Q1 ₂₅ | 25 | 1:0.15 | 1 | 5.0 (5.2, 4.7, <i>n</i> = 2) | 62.2 ± 2.6 (mean ± s.d.; <i>n</i> = 5) | 12.4 |
| Q2 ₂₅ | 25 | 1:0.15 | 2 | 5.5 ± 0.72 (mean ± s.d.; <i>n</i> = 4) | 81.4 ± 5.3 (mean ± s.d.; <i>n</i> = 7) | 14.8 |
| C ₁₀ | 10 | 1:0.15 | 0 | 5.6 | 0 | 0 |
| Q1 ₁₀ | 10 | 1:0.15 | 1 | 5.5 (5.6, 5.3, <i>n</i> = 2) | 62.1 ± 3.0 (mean ± s.d.; <i>n</i> = 5) | 11.1 |
| Q2 ₁₀ | 10 | 1:0.15 | 2 | 5.5 (5.6, 5.4, <i>n</i> = 2) | 86.3 ± 3.0 (mean ± s.d.; <i>n</i> = 3) | 15.7 |
| C _{10A} | 10 | 1:0.08 | 0 | 2.7 | 0 | 0 |
| Q1 _{10A} | 10 | 1:0.08 | 1 | 2.7 | 63.5 (63.8, 63.1, <i>n</i> = 2) | 23.5 |
| Q2 _{10A} | 10 | 1:0.08 | 2 | 2.7 | 70.2 | 26.0 |
| C _{1.8} | 1.8 | 1:0.15 | 0 | 6.4 | 0 | 0 |
| Q1 _{1.8} | 1.8 | 1:0.15 | 1 | 6.4 | 48.1 (48.9, 47.2, <i>n</i> = 2) | 7.5 |
| Q2 _{1.8} | 1.8 | 1:0.15 | 2 | 6.4 | 109 | 17.0 |

the ratios given in Table 1. All other chemicals used in the synthesis of amphiphiles, except organic solvents, were also from Sigma Aldrich, Co., U.K. Organic solvents were purchased from the Department of

Pure and Applied Chemistry, University of Strathclyde, U.K. All chemicals and reagents were used as received. The synthesis procedure is exemplified by the synthesis of C₂₅ (Table 1). PEI (Mw = 25 kDa,

5 g) was reacted with cetyl bromide (1.77 g) by refluxing in tetrahydrofuran (50 mL) for 48 h. Methanol (25 mL) containing NaOH (4.8 g) was added to the above solution, and the resulting solution refluxed for a further 24 h. At the end of the reaction, the sodium bromide salt was filtered off, and the solvent removed by evaporation at 50 °C. The product was dispersed in water (50 mL) and dialyzed against distilled water (5 L) with six changes over 24 h (Visking tubing molecular weight cutoff = 12–14 kDa). The dialyzed product was freeze-dried, and the resulting CPEI (C₂₅) presented as a viscous yellowish liquid.

Synthesis of Quaternary Ammonium Cetyl Poly(ethylenimine) (QCPEI). The synthesis was carried out using a modification of the method reported by Domard and colleagues⁸ (Scheme 1), and CPEI was reacted with over a 1000 molar excess of methyl iodide. The synthesis procedure is exemplified here with the synthesis of Q1₂₅ (Table 1). C₂₅ (600 mg, 0.0185 mmol) was dissolved in methanol (100 mL). Methyl iodide (2.6 mL, 41.8 mmol), sodium hydroxide (229 mg), and sodium iodide (257 mg) were then added to the mixture, and the resulting solution was stirred under a stream of nitrogen for 3 h at 36 °C. At the end of the reaction, the reaction solution was added dropwise to diethyl ether (400 mL), and the precipitate formed was allowed to settle overnight. The supernatant was poured off, and the precipitate was washed with absolute alcohol. The yellow precipitate was then dissolved in a water/alcohol mixture (100 mL:100 mL) and subsequently dialyzed against distilled water with six changes over 24 h. The dialysate was then subjected to an ion exchange procedure over an Amberlite –93 resin column (10 mm × 60 mm) which had been washed with HCL (0.1 M, 100 mL) followed by water until the eluate was neutral in pH. The eluted dialysate was then freeze-dried to give a yellow “cotton-like” solid (Q1₂₅, Table 1). The methylation procedure, described above, was repeated on Q1₂₅ to give Q2₂₅. In the same way, Q1₁₀ and Q2₁₀ were obtained from C₁₀, Q1_{10A} and Q2_{10A} from C_{10A}, and both Q1_{1.8} and Q2_{1.8} from C_{1.8} (Table 1). In the nomenclature used here, Q refers to the quaternary ammonium compounds, the plain font numerals refer to the number of times that the quaternary ammonium reaction was carried out, the subscript numerals refer to the nominal molecular weight, and the letter A indicates that the cetylation was carried out at a lower cetyl bromide to PEI level (Table 1).

Nuclear Magnetic Resonance Analysis (NMR). ¹HNMR, ¹H–¹H COSY, and ¹³CNMR analyses⁴ were performed on all polymers on a Bruker AMX 400 MHz spectrometer, Bruker Instruments, U.K. PEIs (30 mg) and CPEIs (30 mg) were analyzed in deuterated chloroform (1 mL). QCPEIs (35 mg) were analyzed in deuterated methyl alcohol (1 mL).

Elemental Analysis. Elemental analyses were performed on the polymers⁴ using a Perkin-Elmer 2400 analyzer (Perkin-Elmer, U.K.), and this was used to compute the levels of cetylation as previously described⁴ and estimate the levels of quaternization.

Polymer Aggregation and Drug Loading. Preparation of Self-Assembled Polymer Aggregates. Self-assembled polymer amphiphiles were prepared by probe sonication (Soniprep Instrument, U.K.) of PEI amphiphiles in distilled water for 5 min with the instrument set at 75% of its maximum output.

Methyl Orange Probe. Polymer aggregation was probed by the change in the wavelength of maximum absorbance of the colorimetric probe—methyl orange—which undergoes a hypsochromic shift within apolar environments.⁹ Polymer aggregation was thus characterized as reported previously.⁴

Drug Loading. Drug loading was achieved by probe sonication of polymer aggregates in the presence of cyclosporine A (CsA, a gift from Allergan, U.S.A.) in water for 10 min on ice. The formulations were immediately stored at refrigeration temperatures (2–8 °C) or were freeze-dried (Edwards Modulyo Freeze-Drier, Edwards, U.K.) before storage at room temperature (16–25 °C). At various time intervals, the freeze-dried material was reconstituted by vortexing in water, and both the freeze-dried and liquid formulations subjected to HPLC analysis.

Particle Sizing. Isotropic polymer dispersions (5 mg mL⁻¹) were filtered (0.45 μm filter pore size) and sized by photon correlation spectroscopy (Malvern Zetasizer 3000HS, Malvern Instruments, U.K.). Drug-loaded aggregates (polymer/drug ratio = 10 mg mL⁻¹/2 mg mL⁻¹) were also sized by photon correlation spectroscopy without prior filtration. Prior to all sizing experiments, polystyrene standards (mean size = 200 nm, Sigma Co., U.K.) were sized, and the size data obtained agreed with that stated by the manufacturer.

Transmission Electron Microscopy with Negative Staining (TEM). Transmission electron microscopy with negative staining was performed on drug-loaded polymer particles as previously described.¹⁰

HPLC Analysis. Drug-loaded polymer particles were filtered (0.45 μm), the filtrate dissolved in acetonitrile/water (1:1) and subsequently analyzed by HPLC. Samples of the filtrate were analyzed using an HPLC system equipped with a Waters 515 HPLC pump, Waters 717 plus autosampler, and Waters 486 tunable absorbance detector. A reverse-phase column, Waters Asymmetry Spherisorb ODS2 (5 μm, 250 × 4.6 mm), and corresponding Phenomenex Security Guard column C₁₈ (40 × 3 mm) were used, and the column maintained at 80 °C with a Jones Chromatography Column Heater model 7971. The mobile phase was acetonitrile/water/*tert*-butyl methyl ether/phosphoric acid (600:350:50:1) at a flow rate of 1.2 mL min⁻¹. The CsA peak was detected at 210 nm with a retention time of 10.9 min, and the data was analyzed using Waters Empower computer software. A CsA calibration curve was prepared using various standard solutions (0.5–8 μg mL⁻¹, *r*² > 0.99).

Drug recovery (% recovery) from drug–polymer formulations was calculated as shown in eq 1

$$\% \text{ recovery} = 100 \left(\frac{W_c}{W_a} \right) \quad (1)$$

where *W_c* is the weight of CsA detected by HPLC and *W_a* is the weight of CsA loaded in polymer solutions (derived from drug concentrations of 2 mg mL⁻¹ or 30 mg mL⁻¹).

Biological Characterization. Cytotoxicity Assay. The cytotoxicity of PEI and PEI amphiphiles was assessed using the MTT (3-[4,5-dimethylthiazol-2-yl]-2,5-diphenyltetrazolium bromide) indicator dye (Sigma Aldrich, Co., U.K.) assay as previously described.¹¹ All other chemicals and reagents used in the *in vitro* biological characterization of these aggregates were purchased from Invitrogen, U.K. Briefly, Caco-2 cells (American Type Culture Collection, U.S.A.) in an exponential phase of growth were maintained in Dulbecco's Modified Eagle's Medium (DMEM) supplemented with fetal calf serum (FCS, 10% w/v), nonessential amino acids (1% w/v), and L-glutamine (1% w/v), an atmosphere of 10% CO₂, at 95% relative humidity and 37 °C. Cells were seeded (1000 cells well⁻¹) in 96-well microtiter plates and incubated for 72 h. Polymer samples in phosphate-buffered saline (PBS, pH = 7.4) were subsequently incubated with the cells for 4 h; then, the samples were replaced with fresh DMEM medium and the cells incubated for a further 4 days. The MTT indicator dye (50 μL, 5 mg mL⁻¹) was then added to each well and the plates incubated in the dark for 4 h. DMEM and the MTT dye were then aspirated off and DMSO (200 μL) added to dissolve the purple formazan products. Finally, glycine buffer (25 μL; 7.5 g L⁻¹ glycine, 5.9 g L⁻¹ NaCl; pH = 10.5) was added to the wells and the absorbance read at 570 nm (Emax Precision plate reader, Molecular Devices, U.S.A.). Percentage cell viability was expressed relative to the negative control (PBS, pH = 7.4) and the positive control (Triton X-100, 20% v/v).

Transport across Caco-2 Cell Model Epithelia. Caco-2 cells were seeded on Transwell 12-well polycarbonate permeable cell culture inserts (area = 1 cm², pore diameter = 0.4 μm, Corning Life Sciences, U.K.) at a seeding density of 64 000 cells cm⁻². DMEM supplemented with FCS (10% w/v), nonessential amino acids (1% w/v), L-glutamine (1% w/v), penicillin (100 U mL⁻¹), and streptomycin (100 μg mL⁻¹) was used as the culture medium and added to the apical and basolateral compartments of the monolayer, while the cell suspension (0.5 mL)

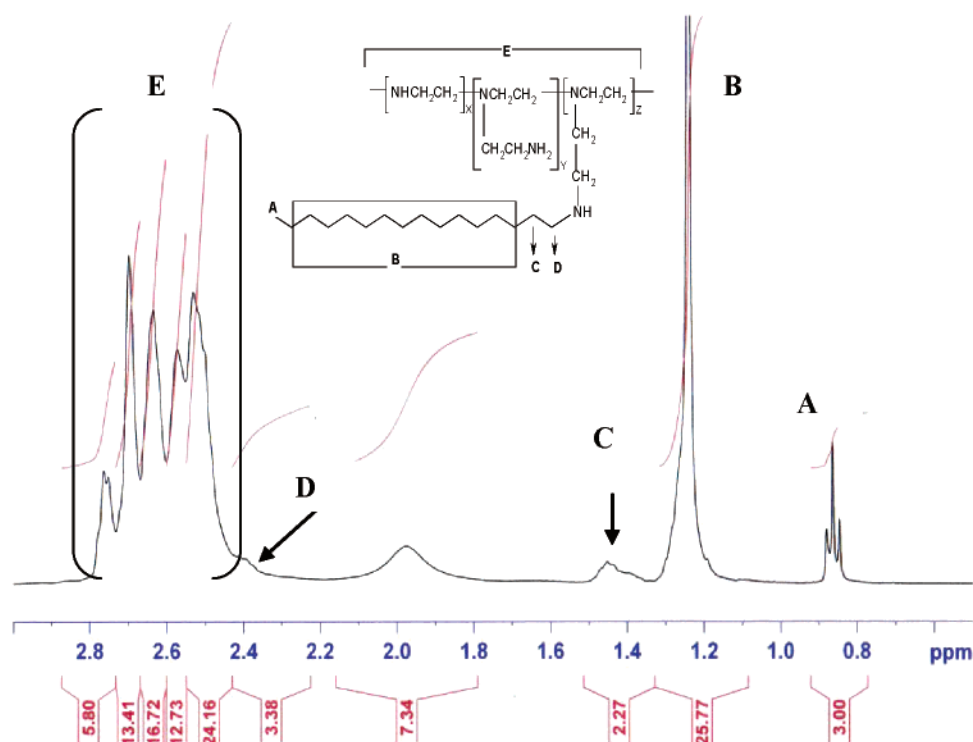


Figure 2. ^1H NMR spectrum of C_{10} in CDCl_3 , signal at $\delta 2.98 = \text{NH}$ peak.

was added to the apical compartments. The plates were incubated at 10% CO_2 , 95% relative humidity, and 37 $^\circ\text{C}$. The medium was changed 3 times a week. Transepithelial electrical resistance (TEER) and transport experiments were then carried out 21–23 days postseeding.

The TEER experiments were carried out using a modification of the method reported by Kotze and colleagues.¹² A Millicell electrical resistance system meter (Millipore, Bedford, MA) connected to a pair of chopstick electrodes was used to measure the TEER of Caco-2 cell monolayers. Polymer solutions (2 and 4 $\mu\text{g mL}^{-1}$) were prepared in Hanks' balanced salt solution (HBSS) containing Ca^{2+} (1.26 nM) and Mg^{2+} (0.9 nM) supplemented with penicillin (100 U mL^{-1}) and streptomycin (100 $\mu\text{g mL}^{-1}$). The HBSS buffer was added into basolateral and apical compartments and the cells incubated at 10% CO_2 , 95% relative humidity, and 37 $^\circ\text{C}$ for 1 h. The TEER of cells was then measured prior to the addition of polymer solutions. Polymer solutions (0.5 mL) were added to apical compartments, and TEER was measured every 40 min, and after 160 min, the polymer solutions were removed. Cells were washed three times and finally replaced with the fresh HBSS buffer. The TEER was measured after 1 h of HBSS buffer incubation to determine the reversibility of the effect of polymer solutions. Control experiments were performed under similar conditions without polymer solutions.

The paracellular transport of Lucifer Yellow (LY), a water-soluble fluorescent dye, was studied to assess the effect of polymer solutions on the integrity of the tight junctions.¹³ Polymer solutions (2 and 4 $\mu\text{g mL}^{-1}$) were prepared in HBSS buffer containing LY (0.4 mg mL^{-1}). HBSS buffer was added to basolateral compartments, and polymer–LY solutions were added to apical compartments. The plates were then incubated at 10% CO_2 , 95% relative humidity, and 37 $^\circ\text{C}$ for 160 min. Samples (1 mL) were taken every 40 min from basolateral compartments and replaced with an equal volume of fresh HBSS buffer. The fluorescent readings of LY in the samples at various time points were measured using $\lambda_{\text{excitation}} = 485 \text{ nm}$ and $\lambda_{\text{emission}} = 530 \text{ nm}$, and the signals were converted to LY concentrations for all samples using standards (2.5–25 $\mu\text{g mL}^{-1}$, $r^2 > 0.99$).

The P-Glycoprotein (P-gp) Efflux Pump. The ability of PEI amphiphiles to inhibit the P-gp efflux pump and thus potentiate the cytotoxicity of doxorubicin was assessed in the A2780AD cell line. A2780 (obtained from Dr. R. F. Ozols, Fox Chase Cancer Centre,

U.S.A.) is a doxorubicin-sensitive ovarian carcinoma cell line, and A2780AD is its doxorubicin-resistant analogue which overexpresses the P-gp efflux pump.¹⁴ Both cell lines were maintained in RPMI 1640 medium supplemented with FCS (10% w/v) and L-glutamine (1% w/v) in 5% CO_2 , at 95% relative humidity and 37 $^\circ\text{C}$. To ensure continued expression of the P-gp pump, A2780AD cells were cultured with doxorubicin (2.0 μM) once every 2 weeks. The MTT assay was similar to the cytotoxicity assay described earlier, except the cells were incubated with various concentrations of doxorubicin alone or doxorubicin in the presence of polymers (2 $\mu\text{g mL}^{-1}$) for 24 h before addition of the MTT dye. The IC₅₀ values for doxorubicin alone or in the presence of polymer solutions were calculated relative to the percentage cell viability observed with negative (PBS, pH = 7.4) and positive (Triton X-100, 20% v/v) controls.

In Vivo Oral Absorption Study. Adult male Wistar rats [(Harlan Olac, U.K.), weight 240–280 g, $n = 4$] were fasted for 12 h before the intragastric administration of CsA (2 mg mL^{-1} , 1 mL, 7.5 or 10 mg kg^{-1}) and for a further 4 h thereafter. CsA was administered either as a dispersion of the drug in water (dispersed by probe sonication), a polymer formulation, or the commercial liquid formulation Neoral (100 mg mL^{-1}), which had been diluted with distilled water to give a solution of 2 mg mL^{-1} . At various time intervals, blood (200 μL) was sampled from the tail vein of anesthetized rats and CsA blood levels analyzed using a monoclonal antibody radioimmunoassay kit (Cyclo-Trac SP-Whole Blood Radioimmunoassay Kit, Diasorin, U.K.) in accordance with the manufacturer's instructions.

Statistical Analysis. Statistical significance was assessed using one-way analysis of variance ANOVA via the statistical software package MINITAB 13.1 for Windows.

Results and Discussion

Polymer Synthesis. PEI was derivatized using cetyl bromide and methyl iodide. The synthesis of PEI amphiphiles was confirmed by ^1H NMR and ^{13}C NMR⁴, and exemplar ^1H NMR spectra are given in Figures 2–4. Further exemplar spectra are given in Supporting Information A and B. ^{13}C NMR signals were assigned, as demonstrated for the ^{13}C NMR of Q2₂₅, as

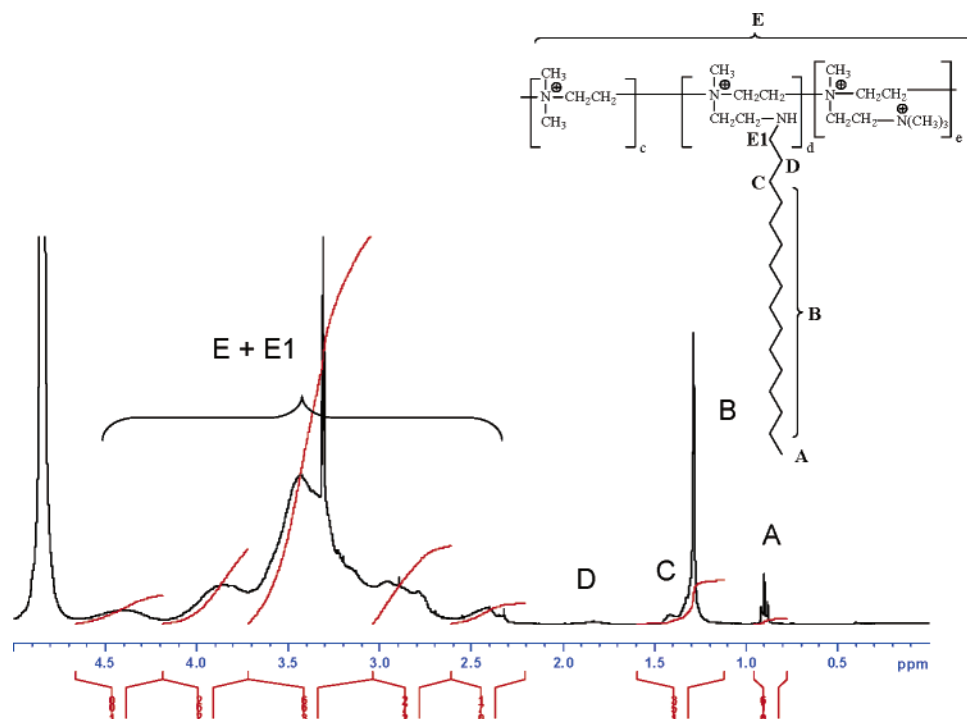


Figure 3. ^1H NMR spectrum of Q1₁₀A in CD₃OD, signals at δ 3.30 and δ 4.84 = solvent peaks.

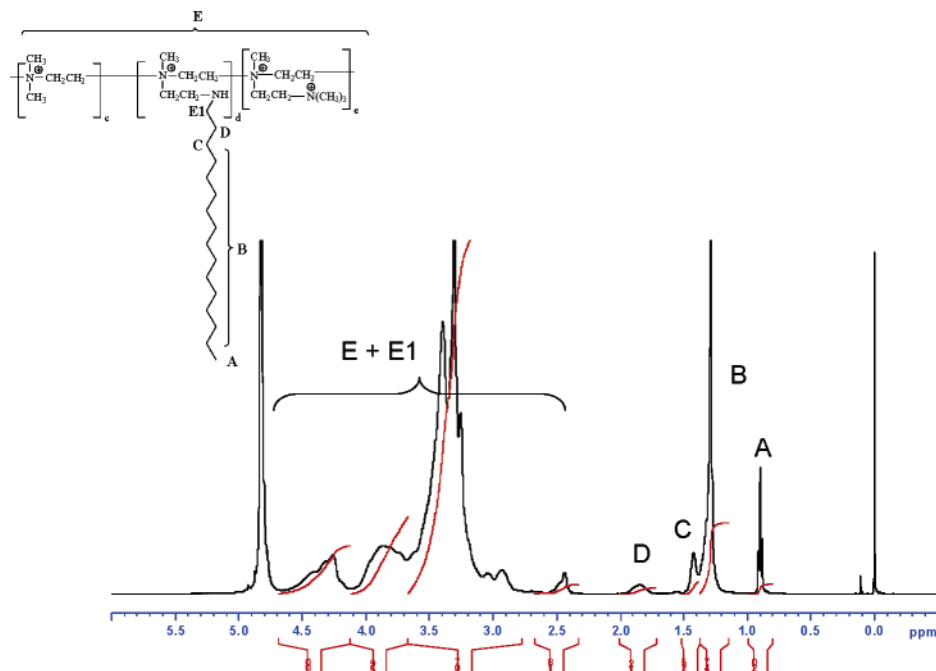


Figure 4. ^1H NMR spectrum of Q2_{1.8} in CD₃OD, signals at δ 3.30 and δ 4.84 = solvent peaks.

follows: δ 14.2 = $\text{CH}_3(\text{CH}_2)_{15}$ (cetyl), δ 23.87, δ 27.89, δ 30.60, δ 32.21 = $\text{CH}_3(\text{CH}_2)_{15}$ (cetyl), δ 52.5, δ 54.8 = $-\text{CH}_2-\text{N}^+(\text{CH}_3)_3$ (PEI) or $\text{CH}_2-\text{N}^+(\text{CH}_3)_2$ (PEI). ^{13}C NMR signals were virtually identical for all other quaternary ammonium amphiphiles. The amphiphiles were obtained in good yield; mean polymer yields were as follows: C₂₅ = 3.3 g ($n = 2$), Q1₂₅ = 702 mg ($n = 5$), Q2₂₅ = 411 mg ($n = 5$), C₁₀ = 4.3 g ($n = 1$), Q1₁₀ = 714 mg ($n = 5$), Q2₁₀ = 492 mg ($n = 2$), C₁₀A = 4.4 g ($n = 1$), Q1₁₀A = 882 mg ($n = 2$), Q2₁₀A = 449 mg, C_{1.8} = 3.6 g ($n = 1$), Q1_{1.8} = 496 mg ($n = 2$), Q2_{1.8} = 378 mg ($n = 1$).

The level of cetylation and quaternary ammonium groups (Table 1) were estimated using elemental analysis as previously

reported for the cetylation of linear PEI;⁴ here, an assumption is made that the derivatized amine groups are actually converted to quaternary ammonium groups, although inevitably, some tertiary amine groups would exist. The level of cetylation, obtained using ^1H NMR data, for C_{1.8}, C₁₀A, C₁₀, and C₂₅ was 6.2, 3.6, 5.6, and 5.4 mol % per monomer. Although there is a slight underestimation of the level of cetylation using NMR data, as the ethylenimine protons overlap with the α -methylene protons of the cetyl group, there is still remarkably good agreement with the data presented above and that given in Table 1. As was previously reported, the level of cetylation is controlled by the initial feed ratio,⁴ and the level of quaterniza-

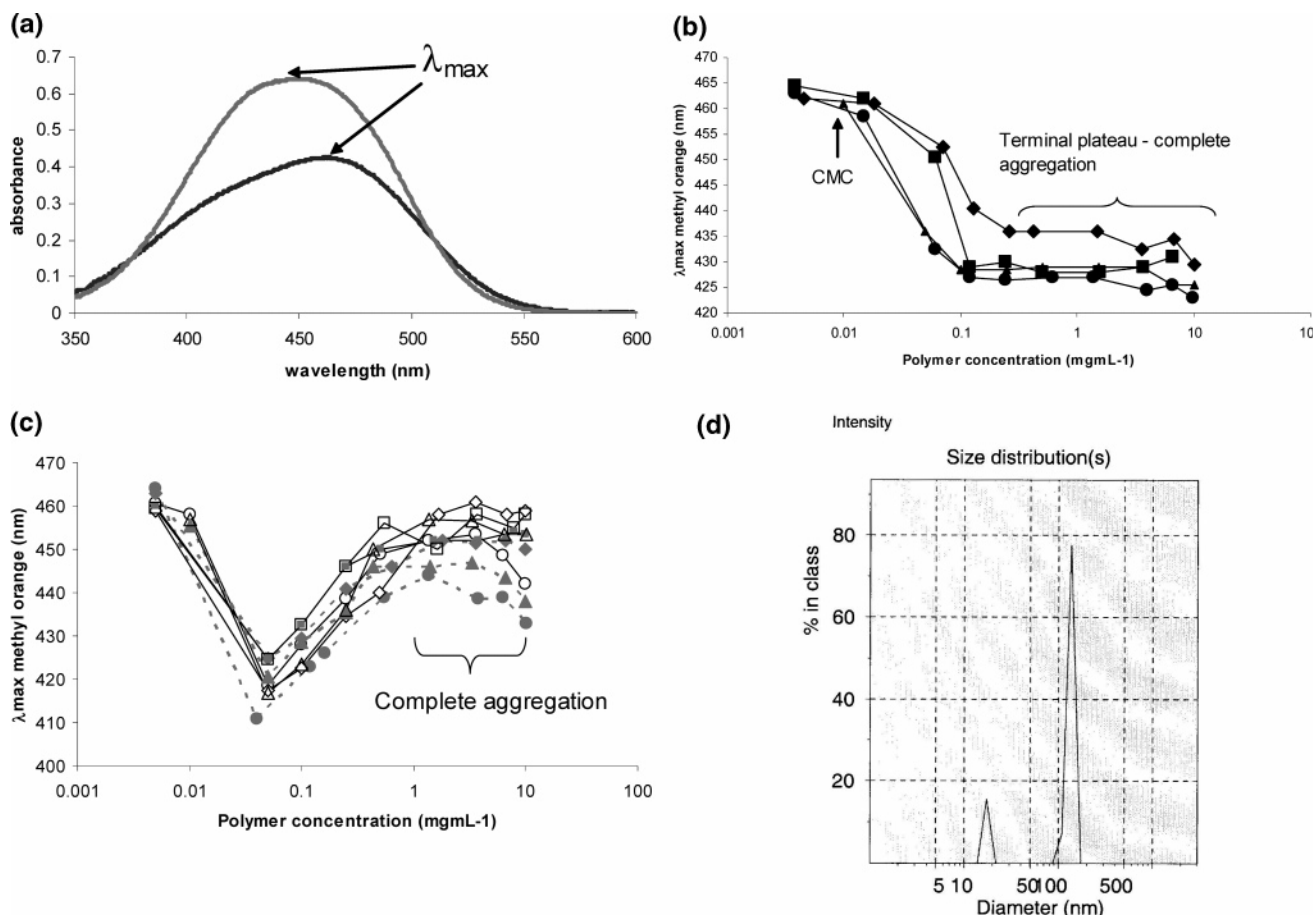


Figure 5. (a) Methyl orange absorption spectra: (black line) = methyl orange (25 μM) in borate buffer; (grey line) = methyl orange (25 μM) in the presence of Q1₂₅ (10 mg mL⁻¹). Data show the methyl orange hypsochromic shift encountered on the methyl orange spectrum: ■ = C₂₅; ● = C₁₀; ◆ = C₁₀A; ▲ = C_{1.8}. (c) The aggregation of quaternary ammonium PEI amphiphiles as evidenced by the hypsochromic shift in the methyl orange spectrum: ■ = Q1₂₅; □ = Q2₂₅; ● = Q1₁₀; ○ = Q2₁₀; ◆ = Q1₁₀A; ◇ = Q2₁₀A; ▲ = Q1_{1.8}; △ = Q2_{1.8}. (d) Particle size distribution of a Q2₂₅ (5 mg mL⁻¹) solution after filtration (0.45 μm).

tion actually achieved is controlled by the number of times that the quaternization procedure was carried out (Table 1). A hydrophilicity index (HI) has been computed (eq 2) as follows:

$$\text{HI} = \frac{Q}{\text{Ct}} \quad (2)$$

where Q = the mol % of quaternary ammonium groups per monomer, and Ct = mol % of cetyl groups per monomer and is used (Table 1) instead of the more commonly used HLB (hydrophilic lipophilic balance), which is usually used for nonionic surfactants³. The HI has been chosen as it specifically refers to the synthetic steps used here.

Polymer Aggregation. All polymers produce isotropic liquids on probe sonication in water, and polymer aggregation is shown by the hypsochromic shift in the methyl orange spectrum^{4,15} (Figure 5a–c). Complete aggregation is indicated by the terminal plateau in the hypsochromic shift–polymer concentration curve (Figure 5b,c). The non-quaternized amphiphiles (Figure 5b) showed a clear inflection in the curve at the start of polymer aggregation and hence a defined critical aggregation concentration (CAC). CAC values were recorded as follows: 0.015, 0.015, 0.010, and 0.018 mg mL⁻¹ for C₁₀, C₂₅, C_{1.8}, and C₁₀A, respectively. However, although it is clear that the quaternary ammonium polymers aggregate in solution, because of the presence of (a) a hypsochromic shift in the methyl orange spectrum and (b) a terminal plateau in the hypsochromic shift–

polymer concentration curve (Figure 5c), the exact CAC of the quaternized amphiphiles is not clearly indicated from these data because of electrostatic interactions between the dye and the polycation below the polymer CAC.¹⁶ These electrostatic interactions produce a pronounced hypsochromic shift ($\lambda_{\text{max}} \leq 420$ nm) below the polymer CAC.

The polarity of the polymer aggregate is controlled at the synthesis step, as demonstrated by the fact that the extent of the hypsochromic shift (420–465 nm) in 10 mg mL⁻¹ polymer solutions is linearly dependent on the polymer HI within each molecular weight class (eqs 3–5)

$$\lambda_{\text{max}} = 1.62\text{HI}_{1.8} + 427 \quad (r^2 = 0.95; n = 3) \quad (3)$$

$$\lambda_{\text{max}} = 1.33\text{HI}_{10} + 421 \quad (r^2 = 0.96; n = 5) \quad (4)$$

$$\lambda_{\text{max}} = 1.67\text{HI}_{25} + 431 \quad (r^2 = 0.999; n = 3) \quad (5)$$

where HI_{1.8} is the hydrophilicity index of polymers in the 1.8 kDa molecular weight class, HI₁₀ is the hydrophilicity index of polymers in the 10 kDa molecular weight class, and HI₂₅ is the hydrophilicity index of polymers in the 25 kDa molecular weight class.

Polymers within the 10 kDa class produce slightly fewer polar aggregates as is shown by the magnitude of the y-axis intercept of the linear equation (eqs 3–5). The intercept may be viewed as the degree of hypsochromic shift that will be obtained at a

Table 2. Particle Size of Polymer Aggregates^a

| sample | PEI amphiphiles alone (10 mg mL ⁻¹) | | | | PEI amphiphile (10 mg mL ⁻¹), CsA (2 mg mL ⁻¹) | | | | | | |
|-------------------|---|-----------------|----------------|-----------------|--|----------------|-----------------|------------------------------|-----------------|------------------------------|-----------------|
| | 25 °C | | 37 °C | | freshly prepared | | | 15 min at 25 °C ^b | | 15 min at 37 °C ^b | |
| | mean size (nm) | poly-dispersity | mean size (nm) | poly-dispersity | initial appearance | mean size (nm) | poly-dispersity | mean size (nm) | poly-dispersity | mean size (nm) | poly-dispersity |
| Q1 ₂₅ | 56 | 0.67 | 43 | 0.77 | clear | | | 559 | 0.42 | 580 | 0.79 |
| Q2 ₂₅ | 96 | 0.71 | 86 | 0.83 | translucent | 288 | 0.36 | 422 | 0.86 | 485 | 0.16 |
| Q1 ₁₀ | 120 | 0.64 | 89 | 0.89 | clear | | | 335 | 0.18 | 508 | 0.87 |
| Q2 ₁₀ | 148 | 0.73 | 100 | 0.79 | translucent | 206 | 0.41 | 251 | 0.21 | 446 | 0.37 |
| Q1 _{10A} | 62 | 0.91 | | | precipitate | | | | | | |
| Q2 _{10A} | 116 | 0.69 | 90 | 0.74 | precipitate | | | | | | |
| C _{1.8} | 25 | 0.46 | | | clear | | | | | | |
| Q1 _{1.8} | 128 | 0.47 | 138 | 0.52 | clear | 171 | 0.19 | 129 | 0.69 | 452 | 0.12 |
| Q2 _{1.8} | 137 | 0.51 | 131 | 0.47 | clear | 161 | 0.41 | 97 | 0.95 | 318 | 0.05 |

^a Size and polydispersity data represent the mean of at least 3 measurements. ^b Samples were stored at 2–8 °C for 3 days prior to exposure to the higher temperature.

limiting HI value (demonstrated by the most hydrophobic polymer in the particular molecular weight class). It is possible that the 10 kDa molecular weight allows both the most flexibility (when compared to the 25 kDa class) and the highest number of hydrophobic groups per molecule (13 cetyl groups per molecule) when compared to the 1.8 kDa class (2.8 cetyl groups per molecule) to enable a high number of hydrophobic associations.

Aggregates are 25–150 nm in size, and aggregates formed from the high molecular weight polymers (MW ≥ 10 kDa) are polydisperse (Table 2). Photon correlation spectroscopy data show two distinct size populations (~20 nm and ~150 nm) in the size distribution plots (Figure 5d), presumably due to the formation of both intra- and intermolecular aggregates, respectively. Increasing the level of quaternization causes a slight increase in particle hydrodynamic diameter. This reduced polymer radius of curvature with increasing quaternary ammonium groups is the consequence of a more extended polymer conformation which arises from intrachain electrostatic repulsions. There was no change in the appearance of the formulations on increase in temperature and no clear trends observed in the particle size data on increase in temperature (Table 2).

Drug Loading. The model hydrophobic drug has a profound effect on polymer self-assembly and gives rise to either micellar liquids with the low HI polymers (HI = 11–12) or larger 200 nm nanoparticles with the intermediate HI polymers (HI = 14–16); while the highest HI polymers (HI = 23–26) show no appreciable drug encapsulation (Table 2, Figure 6). It is clear that a minimum level of cetylation is required for the formation of a hydrophobic domain of sufficient size to solubilize the drug, and hence, stable colloidal aggregates are not formed in the presence of CsA and the highest HI polymers (Q1_{10A} and Q2_{10A}). Aggregate hydrophobic volume is known to be a direct controller of hydrophobic drug encapsulation.^{17,18}

The formation of CsA micellar aggregates (Figure 6a) from the low HI (Q1₁₀ and Q1₂₅) polymers and dense 200–300 nm CsA nanoparticles (Figure 6b) from the intermediate HI polymers (Q2₁₀ and Q2₂₅) originates from the fact that the intermediate HI polymers, with high levels of quaternary ammonium groups, form less hydrophobic cores (Figures 5b,c and 6c) which are insufficiently hydrophobic to solubilize CsA completely at the 2 mg mL⁻¹ level, thus preventing the formation of clear micellar solutions. To reduce the free energy of CsA in aqueous media, there is consequently an increase in polymer aggregation in order to provide a suitable volume of hydrophobic domains. This increase in aggregation number leads to the formation of 200–300 nm nanoparticles (Figure 6b).

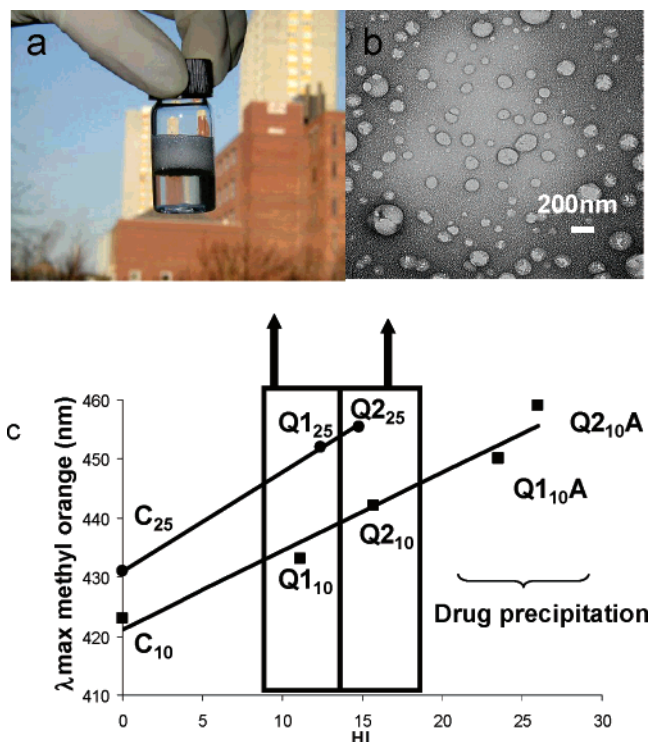


Figure 6. PEI amphiphile/CsA formulations: (a) a freshly prepared solution of CsA/Q1₂₅ containing CsA (2 mg mL⁻¹) and Q1₂₅ (10 mg mL⁻¹); (b) transmission electron micrograph of a CsA/Q2₂₅ containing CsA (2 mg mL⁻¹) and Q2₂₅ (10 mg mL⁻¹) (c) the dependence of the λ_{max} of methyl orange on polymer hydrophilicity index (HI); ● = 25 kDa; ■ = 10 kDa. Isotropic liquids are formed from CsA and the low HI polymers (Q1₁₀ and Q1₂₅ – panel a), while nanoparticles are formed from CsA and the intermediate HI polymers (Q2₁₀ and Q2₂₅ – panel b); the high HI polymers (Q1_{10A} and Q2_{10A}) do not encapsulate drug appreciably (panel c).

The Q2₂₅ and Q2₁₀ formulations increase the aqueous incorporation of CsA by 163-fold and 144-fold per weight fraction of the polymer, respectively, and nanosystems containing 16.7 mg mL⁻¹ CsA in 100 mg mL⁻¹ polymer have been achieved (Figure 7a). This compares favorably with the maximum aqueous drug levels achieved with other amphiphilic polymer systems such as Pluronic F68 (where 0.17 mg mL⁻¹ CsA was solubilized with 22 mg mL⁻¹ of the block copolymer⁶), hydroxypropylmethylcellulose, or dextran amphiphiles (where 0.5–0.8 mg mL⁻¹ CsA was solubilized with 2.5–5.0 mg mL⁻¹ of the polymers^{19,20}). Drug recovery from 2 mg mL⁻¹ CsA liquid formulations was in excess of 75% after 9 months (Figure 7b),

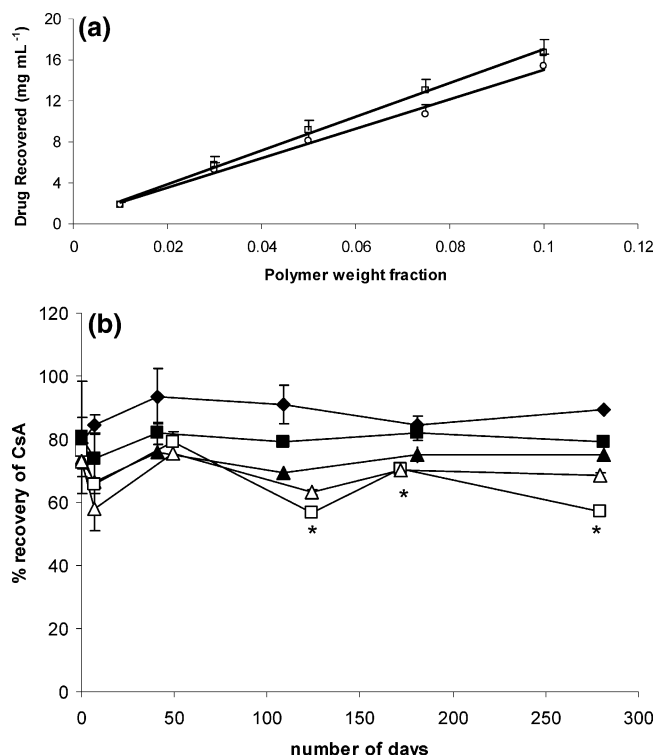


Figure 7. (a) The influence of polymer concentration on drug encapsulation by the polymers; drug recovery is shown as analyzed by HPLC (mean \pm s.d., $n = 3$), $\square = Q2_{25}$, $\circ = Q2_{10}$; initial drug concentration = 30 mg mL⁻¹. (b) Percentage recovery of CsA in PEI amphiphile (10 mg mL⁻¹)/CsA (2 mg mL⁻¹) formulations over a 281-day period. Data represent mean \pm s.d. ($n = 3$). $\blacklozenge = Q1_{25}$ liquid; $\blacksquare = Q1_{10}$ liquid; $\square = Q1_{10}$ freeze-dried; $\blacktriangle = Q2_{10}$ liquid; $\triangle = Q2_{10}$ freeze-dried. * = statistically significant difference from the corresponding liquid formulation ($p < 0.05$).

and drug recovery from the Q2₁₀ formulation was not altered by freeze-drying (Figure 7b).

There is a reversible increase in polymer/drug aggregate size with increase in temperature (Table 2). Micellar aggregates, which present as isotropic liquids, transform to larger nanoparticles (translucent liquids) on standing at 25 or 37 °C, while the nanoparticles formed by the intermediate HI drug-loaded polymers increase in size on increase in temperature (Table 2). The thermal effects noted on drug polymer aggregation are due to the fact that CsA is desolvated in aqueous media on increase in temperature due to intramolecular hydrogen bonding,²¹ thus decreasing the aqueous solubility of CsA with increase in temperature (solubility = 101.5 μ g mL⁻¹ at 5 °C, 19.9 μ g mL⁻¹ at 25 °C, and 3.7 μ g mL⁻¹ at 37 °C⁶). The desolvation of CsA at elevated temperature increases the intermolecular aggregation of the polymers as polymer chains attempt to shield CsA molecules from the aqueous environment and an increase in particle size is observed (Table 2, Figure 8). Hydrophobic molecules have been shown to increase both the aggregation number and the size of PEI amphiphile aggregates;⁴ cooling the translucent formulations results in the reformation of isotropic liquids.

Polymers (10 mg mL⁻¹) in the 1.8 kDa class form isotropic liquids with CsA (2 mg mL⁻¹) due to the formation of micellar aggregates (Table 2), and drug recovery from these formulations was 96%, 71%, and 76% for C_{1.8}, Q1_{1.8}, and Q2_{1.8}, respectively.

Biological Characterization. Oral Absorption Enhancement. The oil-free polymer formulations enhance the oral bioavailability of the encapsulated drug in the rat model (Figure 9a). Bioavailability enhancement was studied at two dose levels. At

the higher dose level of 10 mg kg⁻¹, formulations increased the blood levels of CsA, when compared to the drug dispersed in water (Figure 8a) by between two- and sixfold. However, at this dose level, all of the amphiphiles except C_{1.8} delivered less CsA than Neoral at the 1 h time point only, and high interindividual variability was noted with the C_{1.8} formulation. The absorption of CsA is associated with high interindividual variability due to its absorption being affected by cytochrome P450 enzymes and the gastrointestinal P-glycoprotein efflux pump.²² On the basis of the cumulative (at all time points) percentage of drug blood levels relative to Neoral, the polymers were ranked for absorption enhancement as Q2₁₀ > Q2_{1.8} > C_{1.8} at a CsA dose level of 10 mg kg⁻¹ and Q2₁₀ > Q1₁₀ = Q1₂₅ at a dose level of 7.5 mg kg⁻¹. Polymers with a higher level of methylation were superior absorption enhancers, and polymers in the 10 kDa molecular weight class were also superior to polymers in the 1.8 kDa class. At the lower dose level of 7.5 mg kg⁻¹, drug levels from Q2₁₀ formulations were statistically similar to that seen with the oil-containing micro-emulsion concentrate—Neoral (Figure 9b). Interindividual differences from Q2₁₀ were no different from those obtained with Neoral. These 7.5 and 10 mg kg⁻¹ dose data indicate that the absorption enhancement of Q2₁₀ is saturable in nature. The exact reason for how the polymers' structural features control absorption enhancement requires further study, however.

The current polyelectrolyte formulations were prepared without the aid of nonaqueous solvents such as oils and organic solvents, in contrast with other polymer²³ or lipid²⁴ formulations. All formulations were well-tolerated by the rats with no sign of gross discomfort or toxicity.

Caco-2 Cell Permeability. In an effort to investigate the mechanism by which oral absorption was enhanced, the effect of the polymers on Caco-2 cell monolayer permeability and the P-glycoprotein efflux pump were investigated as detailed below.

Work by Anderberg and others has shown that the MTT assay provides an indirect method of ranking a group of permeability enhancers, as there is a linear correlation between the IC₅₀ in the MTT assay and RC₅₀ (concentration which reduces the transepithelial electrical resistance (TEER) to 50% of its control value) in Caco-2 cell TEER assays.²⁵ A decrease in the TEER indicates an increase in the passive transport of ions across a perturbed monolayer. We thus decided to use the PEI amphiphile MTT data as a coarse and indirect marker of epithelial tight junction integrity, as this avoids the need to measure the monolayer permeability on large proportions of dead or dying cells. Classical permeability and tight junction integrity experiments were used as a fine marker of epithelial permeability at lower concentrations of the polymers.

Since cell densities in both experiments differ and the changes in TEER observed here are reversible, it is impossible to draw conclusions, using the MTT data, on the toxic consequences of the polymers in vivo; not least because the protective nature of the gastric mucus, dilution within the gastrointestinal lumen, and level of free polymer not associated with the aggregate has not been taken into account. For example, it is known that niosome-associated poly(oxyethylene) amphiphiles are not detrimental to Caco-2 cells, whereas similar levels of unassociated polymer are toxic to Caco-2 cells.²⁶ Also, agents such as sodium dodecyl sulfate, which are generally regarded as safe (GRAS) via the oral route,²⁷ show in vitro cell damage via the MTT assay at concentrations found on oral dosing.²⁵ At 0.29 mg mL⁻¹, sodium dodecyl sulfate produces virtually 100% cell death in vitro as measured by the MTT assay.²⁵

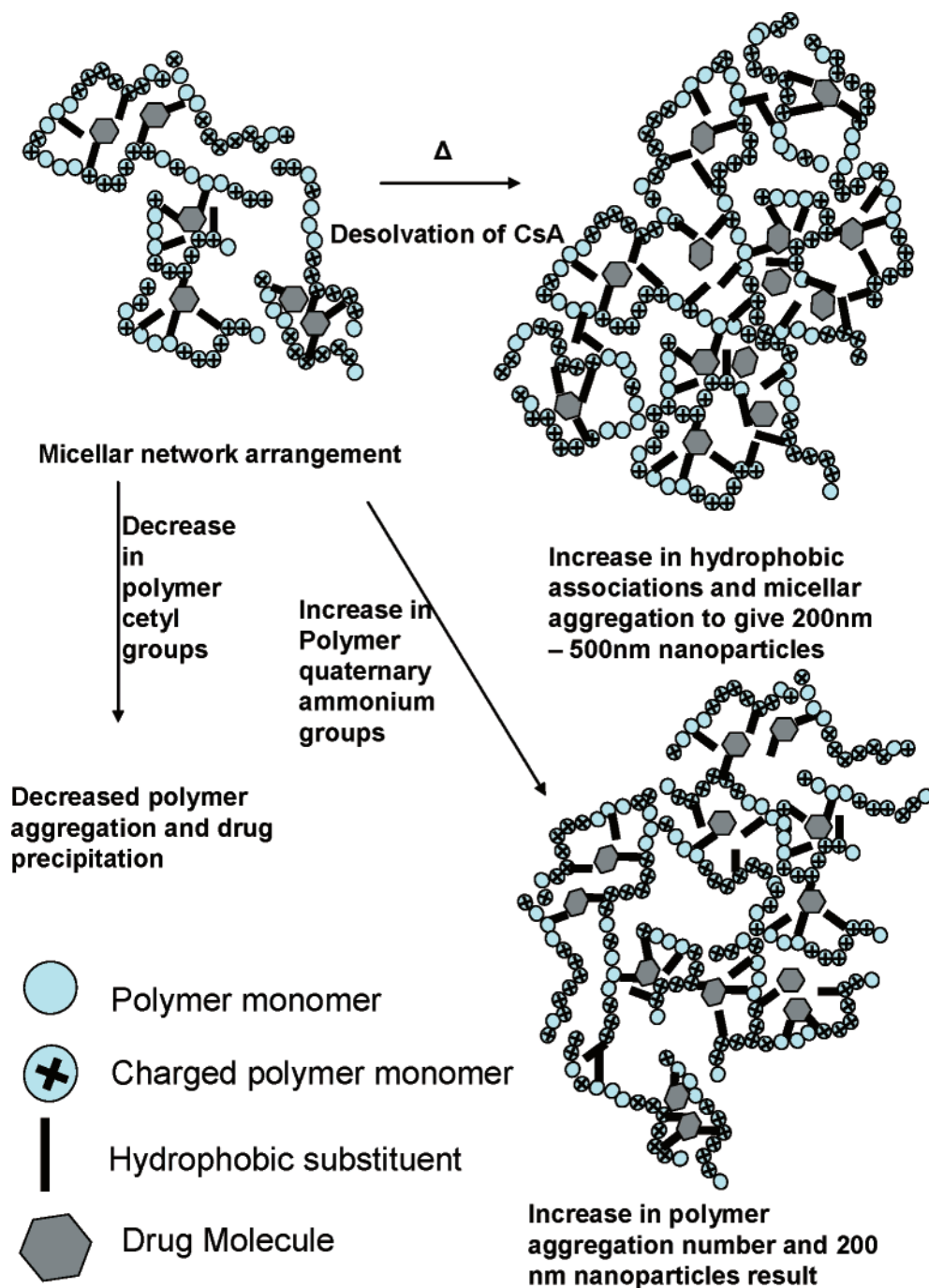


Figure 8. A schematic representation of the formation of nanoparticles (100–300 nm in size) in PEI amphiphile/CsA formulations on increase in temperature or level of PEI amphiphile quaternary ammonium groups.

The IC₅₀ values obtained here after 4 h exposure to cells (Table 3) are lower but comparable to the IC₅₀ values obtained after only 10 min with other amphiphiles, such as sodium dodecyl sulfate (0.104 mg mL⁻¹) and the bile salt, sodium taurodeoxycholate (0.68 mg mL⁻¹), all of which significantly decrease TEER and promote transport across a Caco-2 cell monolayer.²⁵ The IC₅₀ values of the quaternary ammonium polymer amphiphiles in the 10 and 25 kDa class were higher, but only three- to fourfold higher than their parent polymers (Table 3), as has been reported previously.²⁸ It would be expected that the PEIs and PEI amphiphiles would increase the permeability of the Caco-2 cell monolayer in a broadly similar rank order to that shown by the MTT assay,²⁵ i.e., with the parent polymers increasing monolayer permeability to a greater

extent than the quaternary ammonium amphiphile derivatives, and this is indeed the case as detailed below.

To examine the effect of the amphiphiles at low concentrations and directly measure effects on monolayer permeability, the TEER and the permeability of the Caco-2 cell monolayer were studied at polymer concentrations of 2 and 4 μ g mL⁻¹. The TEER values for untreated cell monolayers were 300–350 Ω cm⁻² and similar to literature values.²⁹ All parent PEIs showed a reversible increase in the TEER of Caco-2 cell monolayers at 2 μ g mL⁻¹ (Figure 10a–c). Additionally, the 1.8 and 10 kDa parent PEIs were studied at 4 μ g mL⁻¹, and a reversible increase in TEER was also observed at this higher concentration (Figure 10a–c). Similar TEER effects with high molecular weight PEI (MW = 25 kDa) have been reported.³⁰

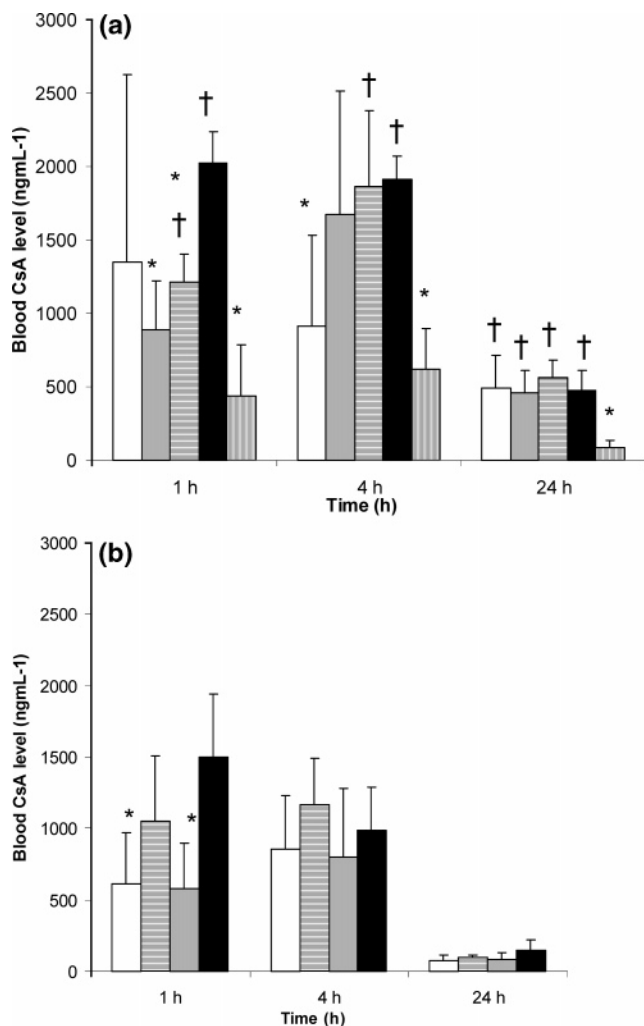


Figure 9. (a) Mean CsA blood levels in rats following oral dosing of CsA (10 mg kg^{-1}) amphiphile formulations (mean \pm s.d., $n = 4$): white bar = $C_{1.8}$; gray bar = $Q_{21.8}$; horizontal-line bar = Q_{210} ; black bar = Neoral; vertical-line bar = CsA suspension. * = statistically significantly less than Neoral ($p < 0.05$); † = statistically significantly higher than CsA suspension in water ($p < 0.05$). (b) Mean CsA blood level in rats following oral dosing of CsA (7.5 mg kg^{-1}) amphiphile formulations (mean \pm s.d., $n = 4$): white bar = Q_{110} ; horizontal-line bar = Q_{210} ; gray bar = Q_{125} ; black bar = Neoral. * = statistically significantly less than Neoral ($p < 0.05$).

Table 3. IC₅₀s of PEIs and PEI Amphiphiles in the Caco-2 Cell Line

| polymer | IC ₅₀ (mg mL^{-1}) |
|--------------------|--|
| PEI (MW = 25 kDa) | 0.0037 |
| Q_{125} | 0.0152 |
| Q_{225} | 0.0127 |
| PEI (MW = 10 kDa) | 0.0045 |
| Q_{110} | 0.0219 |
| Q_{210} | 0.0243 |
| PEI (MW = 1.8 kDa) | 0.0124 |
| $C_{1.8}$ | 0.0061 |
| $Q_{21.8}$ | 0.0138 |

The quaternary ammonium amphiphiles (Q_{225} , Q_{210} , and $Q_{21.8}$) at concentrations of up to $4 \mu\text{g mL}^{-1}$ did not affect the TEER of Caco-2 cell monolayers. Additionally, neither the parent polymers nor the amphiphiles, at a concentration of $4 \mu\text{g mL}^{-1}$, showed a significant effect on the transport of the fluorescent water-soluble paracellular transport marker Lucifer Yellow¹³ (Figure 9b), and although Q_{225} showed an increase in the

transport of this marker, flux data was not significantly different from controls. Normally, a 50% change in TEER values, as opposed to 25% observed here, is required before the transport of a paracellular marker is detected.³⁰

On the basis of these data (MTT and TEER/transport), the quaternary ammonium polymers are less potent in their effects on monolayer permeability than the parent polymers. This is sharply illustrated by considering the decrease in TEER shown by 1.8 kDa PEI and the lack of an effect on TEER shown by $Q_{21.8}$ when both were used at concentrations of 2 and $4 \mu\text{g mL}^{-1}$ (Figure 10a).

Permeability increases are reversible with the parent polymers (Figure 10a–c), and any permeability increases shown by the polymer amphiphiles will, in all probability, also be expected to be reversible. Cationic polymers are known to increase the permeability of Caco-2 cell monolayers,³⁰ and although the direct evidence on gastrointestinal epithelial permeability is not presented, indirect evidence from the MTT assay points to the absorption enhancement observed with the polyelectrolyte amphiphiles in vivo being the result of changes in epithelial permeability. It is thus hypothesized that the oral absorption benefits obtained with these new amphiphiles may be ascribed in part to their effects on gut epithelium permeability.

P-Glycoprotein (P-gp) Assay. The P-glycoprotein (P-gp) efflux pump is localized in the apical membrane of the gastrointestinal epithelium and is responsible for limiting the absorption of xenobiotics such as drugs from the gut lumen^{31–33} by an active transport of any drug back into the gut lumen. CsA is a P-gp substrate,³³ and hence, the inhibition of P-gp by the polymers was probed as a possible mechanism for the promotion of oral absorption. Modulation of P-gp was expressed as the IC₅₀ potentiation index (PI, eq 6)

$$PI = \frac{IC_{50_1}}{IC_{50_2}} \quad (6)$$

where IC_{50_1} is the IC₅₀ of the drug alone in a P-gp expressing cell line and IC_{50_2} is IC₅₀ of the drug plus modulator in a P-gp expressing cell line. As can be seen from Table 4, when the polyelectrolytes ($2 \mu\text{g mL}^{-1}$) were used at a similar level to the well-known P-gp modulator verapamil ($2.8 \mu\text{g mL}^{-1}$), none of the compounds produced a significant PI. It is unlikely that the oral absorption enhancement is due to a modulation of intestinal epithelial P-gp.

General Discussion

Drug absorption of hydrophobic drugs is often limited by their lack of dissolution within sufficient time at the absorptive sites. Usually, dissolution of hydrophobic drugs within the gastrointestinal tract is achieved by the use of organic solvents, polar lipids, surfactants, microemulsions, and cyclodextrins,² and the relevant excipients, which are not always effective, are used at agent-to-drug ratios of at least 15:1, unlike the polyelectrolyte amphiphiles described here. Once dissolution has taken place, there must be transport of the active agent to the blood via paracellular or transcellular mechanisms. Within the 37 °C conditions of the gut lumen, it is assumed that the current polymer formulations will exist as nanoparticles, and we hypothesize that the gradual erosion of these nanoparticles will produce polymer–drug aggregates, which by increasing the local permeability of the gastrointestinal epithelia will promote drug absorption in part via the paracellular pathways. The transcellular pathway is not ruled out, as both PEI particles in

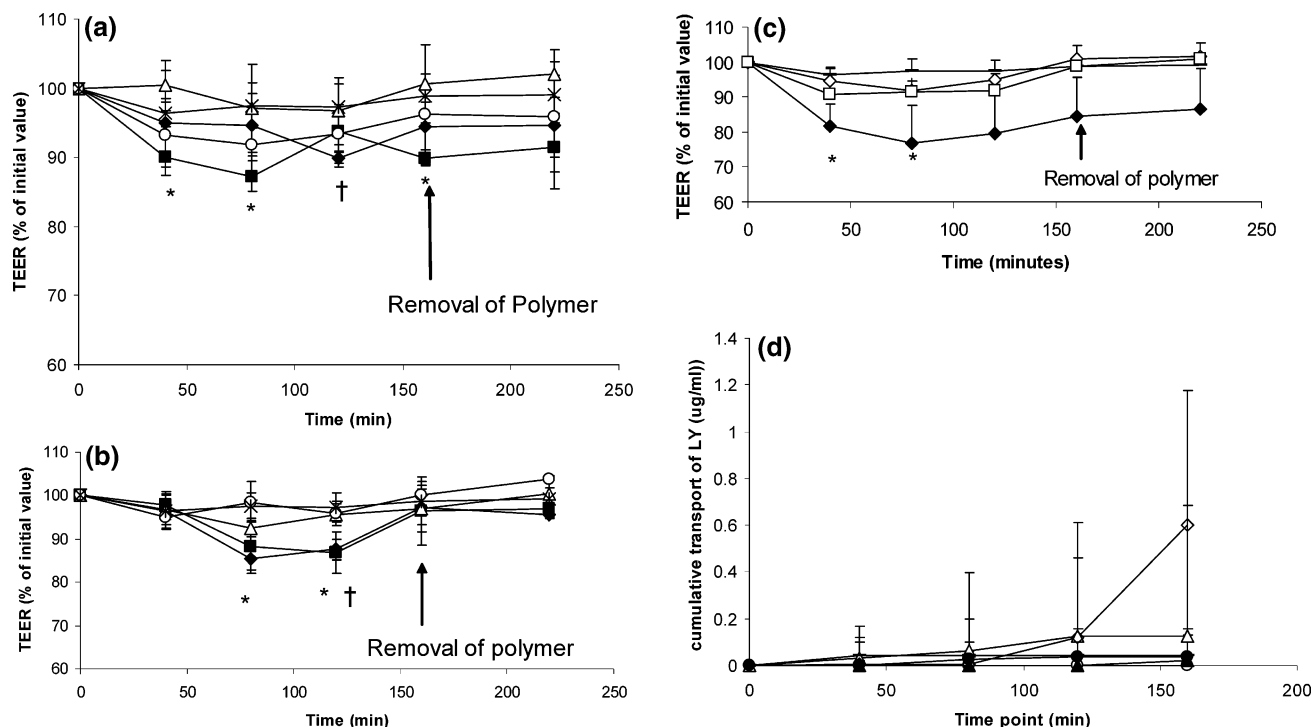


Figure 10. (a) The effect of PEI 1.8 kDa and corresponding amphiphiles on the TEER of Caco-2 cell monolayers; data is mean \pm s.d. ($n = 3$). \blacklozenge = PEI 1.8 kDa (2 $\mu\text{g mL}^{-1}$); \blacksquare = PEI 1.8 kDa (4 $\mu\text{g mL}^{-1}$); \triangle = Q2_{1.8} (2 $\mu\text{g mL}^{-1}$); \circ = Q2_{1.8} (4 $\mu\text{g mL}^{-1}$); \times = control. * = PEI 1.8 kDa (4 $\mu\text{g mL}^{-1}$) statistically significantly lower than control values ($p < 0.05$); \dagger = PEI 1.8 kDa (2 $\mu\text{g mL}^{-1}$) statistically significantly lower than control values ($p < 0.05$). (b) The effect of PEI 10 kDa and corresponding amphiphiles on the TEER of Caco-2 cell monolayers; data represent the mean \pm s.d. ($n = 3$). \blacklozenge = PEI 10 kDa (2 $\mu\text{g mL}^{-1}$); \blacksquare = PEI 10 kDa (4 $\mu\text{g mL}^{-1}$); \triangle = Q2₁₀ (2 $\mu\text{g mL}^{-1}$); \circ = Q2₁₀ (4 $\mu\text{g mL}^{-1}$); \times = control. * = PEI 10 kDa (2 $\mu\text{g mL}^{-1}$) statistically significantly lower than control values ($p < 0.05$); \dagger = PEI 10 kDa (4 $\mu\text{g mL}^{-1}$) statistically significantly lower than control values ($p < 0.05$). (c) The effect of PEI 25 kDa and corresponding amphiphiles on the TEER of Caco-2 cell monolayers; data is mean \pm s.d. ($n = 3$). \blacklozenge = PEI 25 kDa (2 $\mu\text{g mL}^{-1}$); \square = Q2₂₅ (2 $\mu\text{g mL}^{-1}$); \triangle = Q2₂₅ (4 $\mu\text{g mL}^{-1}$); \times = control. * = statistically significantly lower than control values ($p < 0.05$). (d) The effect of PEI amphiphiles and their parent compounds on Lucifer yellow transport across Caco-2 cell monolayers. \blacklozenge = PEI 25 kDa (2 $\mu\text{g mL}^{-1}$); \diamond = Q2₂₅ (4 $\mu\text{g mL}^{-1}$); \bullet = PEI 10 kDa (4 $\mu\text{g mL}^{-1}$); \circ = Q2₁₀ (4 $\mu\text{g mL}^{-1}$); \blacktriangle = PEI 1.8 kDa (4 $\mu\text{g mL}^{-1}$); \triangle = Q2_{1.8} (4 $\mu\text{g mL}^{-1}$); $-$ = control.

Table 4. Effect of PEI and PEI Amphiphiles All Dosed at a Level of 2 $\mu\text{g mL}^{-1}$ on P-Glycoprotein Activity in the A2780AD Cell Line

| sample | cell line | IC50 of doxorubicin ($\mu\text{g mL}^{-1}$) | PI |
|--|-----------|---|-------|
| doxorubicin alone | A2780 | 0.007 | |
| doxorubicin alone | A2780AD | 1.377 | 1.0 |
| PEI 25 kDa | A2780AD | 0.804 | 1.7 |
| Q1 ₂₅ | A2780AD | 1.233 | 1.1 |
| Q2 ₂₅ | A2780AD | 0.789 | 1.7 |
| PEI 10 kDa | A2780AD | 0.840 | 1.6 |
| Q1 ₁₀ | A2780AD | 0.945 | 1.5 |
| Q2 ₁₀ | A2780AD | 1.108 | 1.2 |
| PEI 1.8 kDa | A2780AD | 1.856 | 0.7 |
| C _{1.8} | A2780AD | 0.930 | 1.5 |
| Q2 _{1.8} | A2780AD | 0.262 | 5.3 |
| verapamil (2.8 $\mu\text{g mL}^{-1}$) | A2780AD | 0.053 | 26.0* |

particular³⁴ and polymeric micelles in general³⁵ are known to be taken up by endosomal uptake, and this could result in their translocation across the gut epithelia. It is not clear whether only the drug or the drug and the polymer are able to actually traverse the tight junctions.

In conclusion, solubilizing and absorption-enhancing polyelectrolyte particles may be produced from PEI amphiphiles, and this is the first time that amphiphilic polyelectrolytes have been shown to both solubilize poorly soluble drugs such as CsA and enhance the oral absorption of hydrophobic drugs. Drugs

with both poor oil solubility and poor water solubility may benefit from this approach.

Acknowledgment. W.P.C. was in receipt of Overseas Research and University of Strathclyde studentships. I.F.U. was in receipt of an American Association of Pharmaceutical Scientists New Investigator Grant in Oral Lipid Drug Delivery Systems sponsored by Gattefossé, France.

Supporting Information Available. Additional exemplar spectra. This material is available free of charge via the Internet at <http://pubs.acs.org>.

References and Notes

- (1) Kilpatrick, P. *Nat. Drug Discov.* **2003**, *2*, 337.
- (2) Strickley, R. G. *Pharm. Res.* **2004**, *21*, 201–230.
- (3) Florence, A. T.; Attwood, D. *Physicochemical Principles of Pharmacy*; Macmillan Press: Basingstoke, 1998.
- (4) Wang, W.; Qu, X.; Gray, A. I.; Tetley, L.; Uchegbu, I. F. *Macromolecules* **2004**, *37*, 9114–9122.
- (5) Noble, S.; Markham, A. *Drugs* **1995**, *50*, 924–941.
- (6) Molpeceres, J.; Guzman, M.; Bustamante, P.; Aberturas, M. D. R. *Int. J. Pharm.* **1996**, *130*, 75–81.
- (7) Lucangioli, S. E.; Kenndler, E.; Carlucci, A.; Tripodi, V. P.; Scioscia, S. L.; Carducci, C. N. *J. Pharm. Biomed. Anal.* **2003**, *33*, 871–878.
- (8) Domard, A.; Rinaudo, M.; Terrassin, C. *Int. J. Biol. Macromol.* **1986**, *8*, 105–107.
- (9) Wang, G. J.; Engberts, J. *Langmuir* **1995**, *11*, 3856–3861.
- (10) Wang, Y. Y.; Hong, C. T.; Chiu, W. T.; Fang, H. Y. *Int. J. Pharm.* **2001**, *224*, 89–104.
- (11) Brown, M. D.; Schatzlein, A.; Brownlie, A.; Jack, V.; Wang, W.; Tetley, L.; Gray, A. I.; Uchegbu, I. F. *Bioconjugate Chem.* **2000**, *11*, 880–91.

- (12) Kotze, A. F.; Lueben, H. L.; Boer, A. G.; Verhoef, J. C.; Junginger, H. E. *Eur. J. Pharm. Sci.* **1998**, *7*, 145–151.
- (13) Tsukazaki, M.; Satsu, H.; Mori, A.; Konishi, Y. S.; Shimizu, M. *Biochem. Biophys. Res. Commun.* **2004**, *315*, 991–997.
- (14) Huxham, I. M.; Barlow, A. L.; Lewis, A. D.; Plumb, J.; Mairs, R. J.; Gaze, M. N.; Workman, P. *Int. J. Cancer* **1994**, *59*, 94–102.
- (15) Zhu, D. M.; Wu, X.; Schelly, Z. A. *J. Phys. Chem.* **1992**, *96*, 7121–7126.
- (16) Buwalda, R. T.; Engberts, J. *Langmuir* **2001**, *17*, 1054–1059.
- (17) Zhang, X.; Jackson, J. K.; Burt, H. M. *Int. J. Pharm.* **1996**, *132*, 195–206.
- (18) Shoda, S.; Masuda, E.; Furukawa, M.; Kobayashi, S. *J. Polymer Sci., Part A: Polym. Chem.* **1992**, *30*, 1489–1494.
- (19) Francis, M. F.; Lavoie, L.; Winnik, F. M.; Leroux, J. C. *Eur. J. Pharm. Biopharm.* **2003**, *56*, 337–346.
- (20) Francis, M. F.; Piredda, M.; Winnik, F. M. *J. Controlled Release* **2003**, *93*, 59–68.
- (21) Ismailos, G.; Reppas, C.; Dressman, J. B.; Macheras, P. *J. Pharm. Pharmacol.* **1991**, *43*, 287–289.
- (22) Wachter, V. J.; Salphati, L.; Benet, L. Z. *Adv. Drug Del. Rev.* **2001**, *46*, 89–102.
- (23) Wang, X.; Dai, J.; Chen, Z.; Zhang, T.; Xia, G.; Nagai, T.; Zhang, Q. *J. Controlled Release* **2004**, *97*, 421–429.
- (24) Leigh, M.; Hoogevest, P.; Tiemessen, H. *Drug Delivery Syst. Sci.* **2001**, *1*, 73–77.
- (25) Anderberg, E. K.; Nystrom, C.; Artursson, P. *J. Pharm. Sci.* **1992**, *81*, 879–887.
- (26) Dimitrijevic, D.; Lamandin, C.; Uchegbu, I. F.; Shaw, A. J.; Florence, A. T. *J. Pharm. Pharmacol.* **1997**, *49*, 611–616.
- (27) Rowe, R. C.; Sheskey, P. J.; Weller, P. J. *Handbook of Pharmaceutical Excipients*; Pharmaceutical Press: London, 2003.
- (28) Brownlie, A.; Uchegbu, I. F.; Schatzlein, A. G. *Int. J. Pharm.* **2004**, *274*, 41–52.
- (29) Dimitrijevic, D.; Shaw, A. J.; Florence, A. T. *J. Pharm. Pharmacol.* **2000**, *52*, 157–162.
- (30) Ranaldi, G.; Marigliano, I.; Vespignani, I.; Perozzi, G.; Sambuy, Y. *J. Nutr. Biochem.* **2002**, *13*, 157–167.
- (31) Zhang, Y. C.; Benet, L. Z. *Clin. Pharmacokinet.* **2001**, *40*, 159–168.
- (32) Kruijtzter, C. M. F.; Beijnen, J. H.; Schellens, J. H. M. *Oncologist* **2002**, *7*, 516–530.
- (33) Hunter, J.; Hirst, B. H. *Adv. Drug Delivery Rev.* **1997**, *25*, 129–157.
- (34) Sonawane, N. D.; Szoka, F. C.; Verkman, A. S. *J. Biol. Chem.* **2003**, *278*, 44826–44831.
- (35) Savic, R.; Luo, L.; Eisenburg, A.; Maysinger, D. *Science* **2003**, *300*, 615–618.

BM060130L